Express Polymer Letters Vol.19, No.1 (2025) 94–106
Available online at www.expresspolymlett.com
https://doi.org/10.3144/expresspolymlett.2025.7

Research article

Recyclable high-strength polybutadiene-based rubber with self-healing and shape memory properties via dynamic boronic ester and Diels-Alder chemistry

Shengao Yang[1,2], *Yan Wang*[1,2], *Fang Wang*[3], *Kaiyi Zhang*[1,2], *Xinxin Lv*[1,2], *Hao Teng*[1,2], *Rui Zheng*[1,2], *Faliang Luo*[1,2*], *Qian Xing*[4*]

[1]State Key Laboratory of High-efficiency Utilization of Coal and Green Chemical Engineering, Ningxia University, 750021 Yinchuan, PR China
[2]School of Chemistry and Chemical Engineering, Ningxia University, 750021 Yinchuan, PR China
[3]Institute of Coal Chemical Industry Technology, Ningxia Coal Industry Co., Ltd, CHN Energy Group, Yinchuan, 750411 Ningxia, PR China
[4]School of Light industry Science and Engineering, Beijing Technology and Business University, 100048 Beijing, PR China

Received 9 August 2024; accepted in revised form 16 October 2024

Abstract. Dynamic cross-linked networks (DCNs) endow thermoset rubber with self-healability and recyclability to extend its lifetime and alleviate environmental pollution. However, the contradiction between high self-healing and mechanical properties in DCNs rubber is always difficult to be resolved. Herein, we used boronic ester (BO) and Diels-Alder dynamic covalent bonds (DA) to synthesize polybutadiene-based dual networks rubber (PB-BO-DA) via thiol-ene reaction. This approach achieved a tensile strength of 16.46 MPa and 99% self-healing efficiency, facilitated by extensive intermolecular interactions (π-π packing and N-B coordination) and fully dynamic cross-linking. In addition, multiple dynamic cross-linked networks (MDCNs) polybutadiene-based rubber also show excellent shape memory ability and recyclability. This strategy might open a helpful pathway to fabricate intelligent multifunctional polymers with high strength and high self-healing efficiency.

Keywords: *polybutadiene rubber, dual network, high strength self-healing, recyclable, shape memory property*

1. Introduction

Traditional vulcanized rubber has been extensively applied in the fields of tires, seals, intelligent robots and sensors due to its high elasticity, high ductility and wear resistance [1–5]. However, conventional thermosetting rubber containing three-dimensional cross-linked networks cannot be reshaped and reprocessed like thermoplastic resins, and they are difficult to recycle by melting or dissolving once formed. Incineration and landfill treatment of the waste rubber has also brought about environmental pollution and energy waste [6]. In recent years, inspired by the self-healing capabilities of living organisms, a variety of strategies have been developed for the fabrication of self-healing materials of different functionalities. One of the most interesting strategies involves the fabrication of self-healing rubber with thermoplastic and recyclable properties. This approach relies on reversible noncovalent supramolecular interactions or dynamic covalent bonds, which form dynamic cross-linked networks (DCNs) [3, 5, 7–10]. At present, noncovalent supramolecular interactions (hydrogen bond [7, 8], ion interaction [9], metal-ligand coordination [10, 11], π-π packing

---

[*]Corresponding author, e-mail: fll@nxu.edu.cn (Faliang Luo);
xingqian@btbu.edu.cn (Qian Xing)

[12, 13], *etc.*) and dynamic covalent bonds (disulfide bond [14, 15], imine bond [16, 17], boronic ester (BO) transesterification [16, 18], Diels-Alder bond (DA) [19, 20], *etc.*) have been simultaneously used as candidates for the construction of self-healing rubber [21]. Wu *et al.* [22] designed a high mechanical strength, transparent, self-healing elastomer with covalent cross-links and reversible hydrogen bonds by random branching method. However, the elastomer showed only 30% self-healing efficiency and a tensile strength of only 4 MPa. Yang *et al.* [23] successfully introduced imine and N-coordination boronic ester dynamic bond into polybutadiene rubber, achieving a high tensile strength of 12.35 MPa. However, the material exhibited only 60% self-healing efficiency. Zhao *et al.* [24] developed a dual network polydimethylsiloxane (PDMS) elastomer by introducing imine bonds and thermal corresponding DA. This elastomer achieved a 99% self-healing efficiency; however, the self-healed tensile strength was only 1.04 MPa. Despite extensive research, intrinsic self-healing approaches reported to date do not fully meet the requirements for industrial applications, as they lack straightforward fabrication methods that achieve both high mechanical performance and effective self-healing capabilities. Therefore, developing rubber that balances good self-healing ability and strength remains a crucial scientific and engineering challenge.

In this work, we utilize various noncovalent supramolecular interactions and dynamic covalent bonds to form multiple dynamic cross-linked networks (MDCNs). This approach achieves a tensile strength of 16.46 MPa, the highest reported to date, along with a 99% self-healing efficiency. Therefore, benzene and diphenyl were designed to form π-π stacking, with coordination bonds between electron-rich nitrogen in amines and electron-deficient B-atom in boronic ester bonds to act as sacrificial bonds to provide rapid self-healing ability. Meanwhile, boronic ester exchange and Diels-Alder dynamic covalent bonds were incorporated to fulfill a cross-linking role, ensuring the material's high strength, which was achieved by introducing benzene-1,4-diboronic acid and bismaleimide onto polybutadiene chain through a thiol-ene reaction. The π-π stacking, coordination bonds, boronic ester exchange and Diels-Alder bonds were characterized and their effects on the properties of polybutadiene were discussed. Additionally, dynamic bonds generally can endow polymer reprocessing and shape memory ability by altering the topological structure of polymer networks. Therefore, the reprocessing ability and shape memory of polybutadiene-bonded benzene-1,4-diboronic acid and bismaleimide were also investigated.

2. Materials and methods

2.1. Materials

1,2-Polybutadiene (PB, approximately 90% 1,2-vinyl, M_w = 5.3 kg/mol, polydispersity index (PDI = 1.2) was purchased from Sigma-Aldrich Trading Co., Ltd (Shanghai, China). 1-thioglycerol (98%), benzene-1,4-diboronic acid (98%), furfuryl mercaptan, bismaleimide (BMI), 2,2-dimethoxy-2-phenylacetophenone (DMPA), anhydrous magnesium sulfate ($MgSO_4$) was purchased from Aladdin Biochemical Technology Co., Ltd (Shanghai, China). Reagents and solvents were used as received without purification.

2.2. Synthesis of 2,2′-(1,4-phenylene)-bis[4-mercaptan-1,3,2-dioxaborolane] (BDB)

BDB was synthesized according to previous work [16–18, 23]. Dithiol-containing boronic ester was used as a cross-linker and was synthesized from the complexation between benzene-1,4-diboronic acid and 1-thioglycerol. Briefly, benzene-1,4-diboronic acid (3.0 g, 18.1 mmol) and 1-thioglycerol (4.01 g, 37.1 mmol) were dissolved in tetrahydrofuran (80 ml) containing 0.1 ml water, then magnesium sulfate of 5.0 g was added. After stirring at room temperature for 24 h, the mixture was filtered and concentrated. Then, the solid obtained by repeated filtration and washing with rich *n*-heptane was concentrated to obtain the target compound as a white solid (5.0 g, 88%).

2.3. Preparation of furan functionalized polybutadiene

The synthesis of furan functionalized polybutadiene (PB-yFu) was carried out as previously described [25]. PB-yFu is the product of the functionalization of polybutadiene (PB) by furfuryl alcohol, and y is the mole fraction of furfuryl alcohol relative to the total number of PB monomer units. Taking PB-4Fu as an example, furfuryl mercaptan (0.51 g), PB (6 g, 0.11 mol) and 30 mg photoinitiation agent (DMPA) were dissolved in a round-bottom flask containing 30 ml CH_2Cl_2 and then reacted with 365 nm ultraviolet irradiation for 3 h under magnetic stirring at room temperature. Finally, the butadiene unit with a 4% molar fraction of PB reacts with furfuryl alcohol. The degree of functionalization was calculated by H nuclear magnetic resonance spectra (^{1}H NMR).

As shown in Table 1, the data of integrals which were used to calculate the mount of grafted furan groups was added in supporting information. The peak at $\delta = 3.68$ was the signal of the proton connecting to the carbon atom between furan ring and sulfur. The peak at $\delta = 4.94$ and signal between 4.94 and 5.25–5.68 belong to hydrogen bonding protons connected to 1,2-butadiene and 1,4-butadiene, respectively. As shown in Equation (1), the integrals S_4, S_1 and S_{2+3} of peak $\delta = 3.68$, $\delta = 4.94$ and $\delta = 5.25–5.68$ were used to calculate the grafting ratio (R_f) of furan groups:

$$R_\mathrm{f} = \frac{2S_4}{S_1 + 2S_{2+3} + 2S_4} \tag{1}$$

Table 1. Theoretical and experimental values of furan grafting ratio.

Theoretical grafting ratio	S_1	S_{2+3}	S_4	Experimental grafting ratio
2%	1	0.709	0.023	1.87%
4%	1	0.720	0.049	3.86%
6%	1	0.721	0.075	5.79%
8%	1	0.724	0.103	7.76%

2.4. Preparation of PB-*x*BO-*y*DA flims

For PB-*x*BO-*y*DA, *x* and *y* represent the percentage of dynamic boronic ester and Diels-Alder bonds and butadiene units in PB chain, respectively. 6 g PB-*y*Fu and *y*/2 BDB were added to a round-bottom flask containing 40 ml toluene, and 30 mg of photoinitiation agent (DMAP) was added under stirring evenly. Then, the polybutadiene PB-BO single network was initially cross-linked by 365 nm ultraviolet irradiation for 30 min under magnetic stirring at room temperature. Finally, the BMI of *y*/2 was added to the above 40 ml PB toluene solution and reacted at 90 °C for 4 h to make the DA reaction fully carried out. The PB-*x*BO-*y*DA mucus was poured into the polytetrafluoroethylene mold to slowly evaporate the toluene and dried in a vacuum oven for 48 h until the quality remained unchanged.

2.5. Characterization

^{1}H NMR spectra were carried out on a Bruker Avance 400 MHz spectrometer (Bruker Corporation, Massachusetts, USA) with $CDCl_3$ (^{1}H, $\delta = 7.26$) as the solvent and tetramethylsilane (TMS) as an internal standard at room temperature.

Fourier transform infrared spectra (FTIR) were acquired using a Bruker VERTEX 70v spectrometer (Bruker Corporation, Massachusetts, USA) with KBr pellet technique in attenuated total reflectance (ATR) mode), from 400 to 4000 cm^{-1}. Variable temperature FTIR measurements were carried out on a Thermo Scientific Nicolet™ iS50 device (Thermo Fisher Scientific Inc., USA), with a temperature rise rate of 5 °C/min.

Thermogravimetric analyses (TGA) were carried out in Ar atmosphere using 30 to 800 °C using a NETZSCH STA 449 F (Netzsch GmbH & Co. KG, Selb, Germany) thermal analyzer to record the weight loss curve of the sample during heating. The temperature range was from 30 to 800 °C at a heating rate of 5 °C/min.

Glass transitions of the materials were determined on an TA Instruments Q20 (TA Instruments, Delaware, USA) differential scanning calorimeter (DSC). Samples were heated from room temperature to 90 °C to remove the residual solvent, followed by a temperature ramp sequence (cooling, heating) at 10 °C/min in the range of –50 to 150 °C under a nitrogen atmosphere. The device was calibrated with sapphire and high purity indium metal. All samples were prepared in a sealed pot (5–10 mg/sample) and compared with an empty pot.

Dumbbell shape samples were tested on a UTM4203 device (Shenzhen SUNS Technology Stock Co., Ltd., Shenzhen, China) at a fixed cross-head speed of 100 mm/min for uniaxial tensile testing. All materials were tested at room temperature. Following the tensile test, the vitreous sample was cut into small pieces and reshaped by compression molding for 30 min at 150 °C under a load of 10 MPa in order to test its recyclability in several reprocessing cycles. The recycling efficiency in terms of tensile strength was represented by η_r (Equation (2)):

$$\eta_\mathrm{r}\,[\%] = \frac{\sigma_\mathrm{reprocessed}}{\sigma_\mathrm{virgin}} \cdot 100 \tag{2}$$

where $\sigma_\mathrm{reprocessed}$ is the tensile strength measured after the recycling process, and σ_virgin is the tensile strength of the original material.

For self-healing tests, dumbbell shape samples were cut into 2×2 mm cross scratches at the neck via a scalpel. After healing at 150 °C for 30 min and 80 °C for 120 min, the healed samples were then subjected to tensile tests at room temperature. Self-healing efficiency (η_s) was calculated from the ratio of the tensile strength of the healed samples (σ_{healed}) to that of the virgin samples (σ_{virgin}) (Equation (3)). Each measurement was repeated at least five times, and the values were averaged.

$$\eta_s\,[\%] = \frac{\sigma_{\text{healed}}}{\sigma_{\text{virgin}}} \cdot 100 \tag{3}$$

The self-healing wounds treated at 80 and 150 °C were observed by an Olympus BX-53P polarizing microscope (POM, Olympus Corp., Tokyo, Japan). The π-π stacking was verified further by the density functional theory (DFT) calculations. All DFT calculations have been carried out by the latest version of ORCA quantum chemistry software version of 5.0.4 (FACCTs GmbH, Köln, Germany). The M06-2X functional with Grimme's DFT-D3 dispersion correction was adopted for all calculations. For geometry optimization calculations, the def2-SVP basis set was used, and the optimal geometry for each compound was determined. The singlet point energy calculations were performed with def2-TZVP basis set. Based on the optimized structure, independent gradient model (IGM) analysis based on Hirshfeld partition of molecular density (IGMH) wave function analysis was performed using Multiwfn software to more clearly show the interaction between molecules. The iso-surface map was rendered by VMD 1.9.3 software. The change in Gibbs free energy (ΔG) between BDB and Diels-Alder adduct was calculated by Equation (4):

$$\begin{aligned}\Delta G = {} & \Delta G_{\text{BDB + Diels − Alder adduct}} - \\ & -\left(\Delta G_{\text{BDB}} + \Delta G_{\text{Diels − Alder adduct}}\right)\end{aligned} \tag{4}$$

Dynamic mechanical analyses (DMA) were conducted on a TA Instruments Q850 device (TA Instruments, Delaware, USA) in tension mode. Heating ramps were performed from –50 to 150 °C at a constant rate of 3 °C/min with a maximum deformation of 30 µm a fixed frequency of 1 Hz.

The folding/unfolding experiments were also used to evaluate shape memory behavior. Shape memory process of the resulting polymer was monitored using a digital camera. The rectangle samples were deformed to a temporary shape at 90 °C first and then fixed the temporary shape until cooling to –20 °C. Afterwards, the deformed sample was heated again at 90 °C to recover the original shape.

3. Results and discussion

3.1. Construction and characteristics of dual-dynamic PB-*x*BO-*y*DA network

The polybutadiene dual network prepared by boronic ester and DA bond is shown in Figure 1, 2,2′-(1,4-phenylene)-bis[4-mercaptan-1,3,2-dioxaborolane] (BDB) and furfuryl mercaptan with mercaptan groups reacted with double bonds in PB through a photo-initiated thiol-ene chemistry reaction to generate the first cross-linked network. Subsequently, the Diels-Alder reaction with BMI was performed at 90 °C to generate the second cross-linked network.

Following the design mechanism, a series of samples with adjustable mechanical properties were synthesized by simply controlling the ratio of the two networks. The stepwise polymerization allowed the two networks to interpenetrate each other and produced a translucent polybutadiene rubber. It can be deduced that a large number of intermolecular π-π packing and N-B coordination bonds between the two networks can easily dissociate and regenerate, dissipating a large amount of energy during deformation.

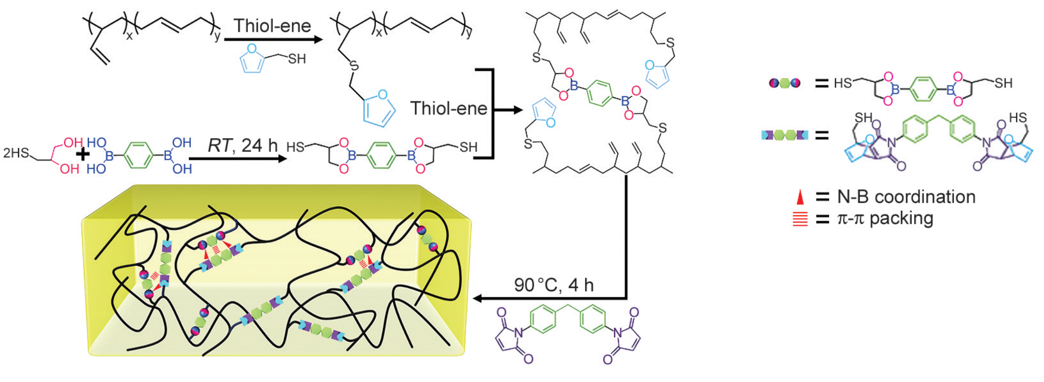

Figure 1. Synthesis of BDB, PB-*y*Fu and PB-*x*BO-*y*DA.

When the temperature was lower than the temperature of dissociating Diels-Alder bonds (r-DA), the exchange of boronic ester could further dissipate energy, while the DA bond served as a cross-linking site that helps maintain the shape of the material. When the temperature exceeds the dissociation temperature of Diels-Alder bonds, the exchangeable boronic ester bonds can cross-link with polybutadiene to maintain its fundamental solid-state properties.

In order to verify the occurrence of thiol-ene and Diels-alder reactions, the FTIR spectrum was tested. As shown in Figure 4c, in the pure PB sample, peaks at 1640 cm^{-1} corresponded to the cis/trans stretching vibration peaks of 1,4-butadiene. Peaks at 909 and 994 cm^{-1} indicated the 1,2-butadiene stretching vibration, while 1450 cm^{-1} corresponded to the C–H stretching vibration peak of $–CH_2–$. After cross-linking, the spectrum of PB-8BO exhibited two characteristic peaks at 1212 and 1314 cm^{-1}, corresponding to the stretching vibration peak of the dynamic B-O bond and the absorption peak of the B-C bond, respectively. In PB-8DA, three distinctive peaks appeared at 1707, 1187 and 1147 cm^{-1}, representing the C=O carbonyl stretching vibration in BMI, the DA ring formed by Diels-Alder reaction and the C–O–C in the furan group, respectively.

By changing the content of dynamic B-O and DA-bonds, dual network PB rubber with different compositions was prepared. Further FTIR analysis showed that when the dynamic B-O bond content was fixed at 8 wt%, the stretching vibration peak of C=O at 1707 cm^{-1} and the characteristic absorption peak of the DA ring at 1187 cm^{-1} also increased with the increase of the dynamic DA bond. When the dynamic DA bond content was fixed at 8 wt%, as the dynamic B-O bond content increased, the B-C bond absorption peak intensity corresponding to 1314 cm^{-1} also increased. Therefore, we have dynamically adjusted the mechanical strength of the polybutadiene dual network by changing the content of BDB and DA, respectively.

3.2. Thermodynamic analysis

The TGA curves of polybutadiene-based dual networks rubber (PB-BO-DA) is shown in Figure 2a. It can be seen that the initial weight loss temperature of PB-BO-DA is 200 °C, and the temperature at which the material loses 5% weight ($T_{d5\%}$) is 215 °C, indicating that the material has excellent thermal stability. This also provides a prerequisite for the material to be multiple times thermally reprocessed.

As is well known, the glass transition temperature (T_g) is the lowest temperature at which polymer chains can move, and it is positively correlated with the cross-linking density of the polymer. It can be seen from Figure 2b, the T_g of PB-8BO at –6.98 °C was significantly higher than that of PB-8DA at –21.27 °C, showing a great enhancement of the cross-linking density of PB-8DA. This enhancement results from the dynamic changes in cross-linking density during the dissociation and reformation of the DA bond (r-DA and DA). Moreover, PB materials containing dynamic B-O bonds showed higher T_g, indicating that dynamic B-O bonds imposed stronger constraints on polymer chains.

As can be seen from Figures 2c and 2d, an endothermic peak between 90 to 150 °C appeared on the heating curve of PB-8DA, indicating the occurrence of r-DA reaction and the fracture of DA cross-linking network. When the contents of B-O and DA bonds were fixed separately, it was observed that T_g increased more significantly with an increase in B-O bond content. At an 8% content for both B-O and DA bonds, T_g reached a maximum value of 19.88 °C. Furthermore, when the content of B-O bond was constant, the r-DA heat absorption peak increased with the increase of DA bond content. When the content of DA bond was constant, the strength and enthalpy of the r-DA endothermic peak gradually decreased with increasing B-O bond content. This trend suggested that higher B-O bond content enhanced the r-DA reaction while potentially reducing the constraint on polymer chains, which could compromise self-healing efficiency.

3.3. Self-healing properties

According to previous reports [6, 9, 15–20], the self-adhesive properties are evident in unvulcanized rubber due to the diffusion ability of the rubber chains, but these properties disappear in vulcanized rubber. The dual dynamic bond network PB shows excellent mechanical properties at room temperature and efficient self-healing ability at high temperatures. To visually illustrate the self-healing capability of PB-BO-DA rubber, dumbbell samples were cut with an ultra-thin blade (Figure 3a and 3d, and the healing of scratches at high temperatures was observed with a POM. As shown in Figure 3b and 3e, the scratches

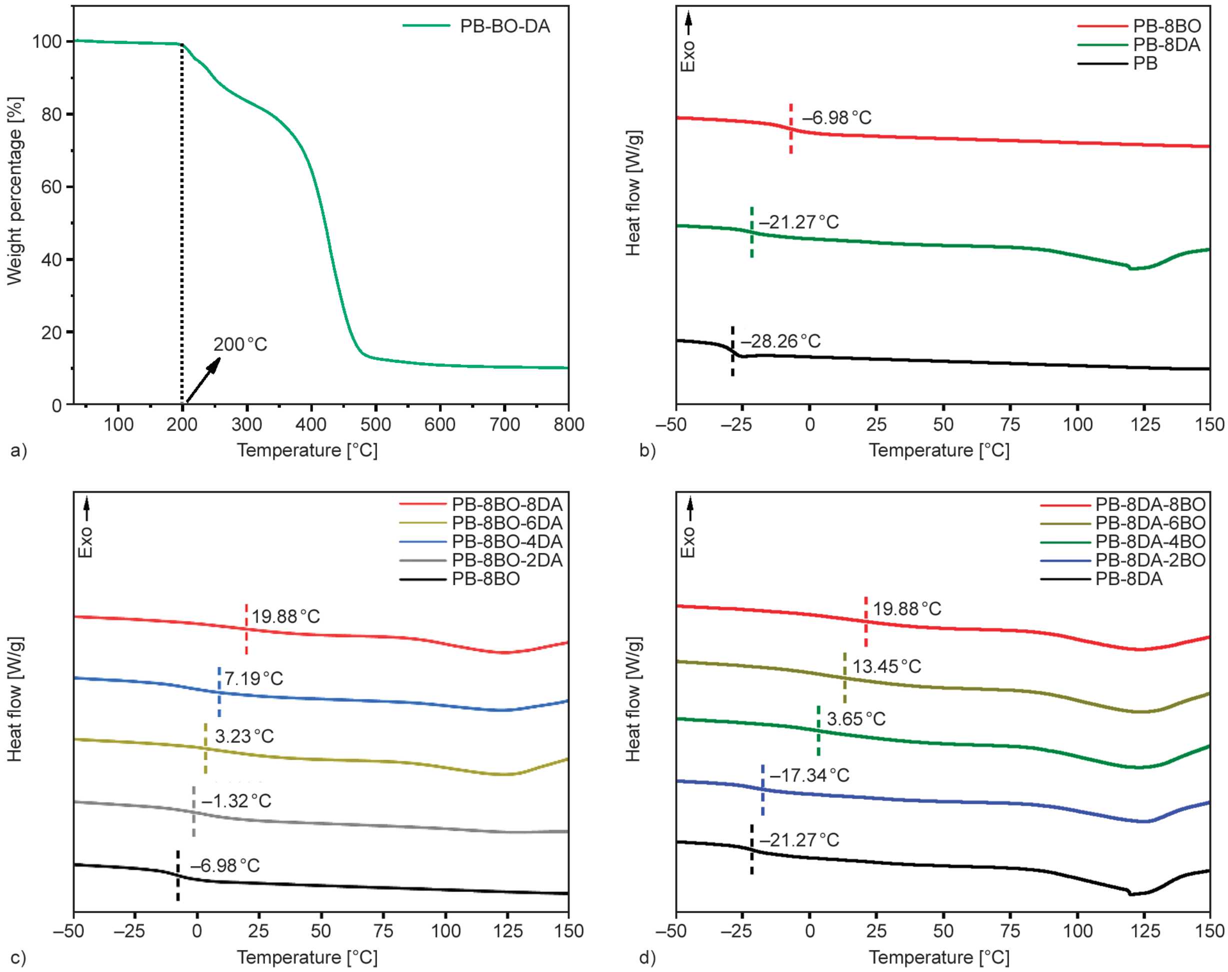

Figure 2. a) TGA curves of PB-BO-DA, b) DSC curves of PB with PB-8BO and PB-8DA, c) DSC curves with different DA contents at PB-8BO, d) DSC curves with different BO contents at PB-8DA.

of PB-8BO-8DA began to re-bond the cutting surface at 80 °C for 30 min due to the exchange reaction of dynamic B-O bonds within the scratches. Further, the fully healed scratches were obtained after treatment at 150 °C for 30 min and at 80 °C for 120 min (Figure 3c and 3f). This complete healing process was facilitated by the activation of all dynamic bonds through the r-DA reaction at 150 °C, followed by the re-exchange of DA reactions and B-O bonds at 80 °C to ensure thorough reaction completion.

Currently, there is no standardized method for assessing self-healing efficacy. Self-healing efficiency was calculated based on the ratio of breaking strengths between healed and uncut samples. By comparing the tensile curves before and after healing (Figures 4a and 4b), a maximum tensile strength of 16.46 MPa and a self-healing efficiency exceeding 99% were observed. In particular, the elastic region of the healed sample was almost the same as that of the original sample, and the healing efficiency remained consistent even with increased cross-linking density. Detailed mechanical properties and self-healing efficiencies for the PB-BO-DA series materials are provided in Table 2.

The scratch self-healing process was also detected by variable temperature FTIR, and the results were shown in Figure 4c. Taking PB-8BO-8DA as an example, there was no significant change when the temperature rises to 80 °C. However, upon further heating to 150 °C, the stretching vibration peak of carbonyl (–C=O) in the DA bond shifted from 1707 to 1717 cm^{-1}. In addition, the characteristic absorption peak of the Diels-Alder adduct ring imide bond at 1187 cm^{-1} almost disappeared [26, 27]. However, these changes reverted when the temperature returned to its initial level after reaching 150 °C and then dropping back to 80 °C. Variable temperature FTIR results indicated the presence of numerous intermolecular interactions, such as hydrogen bonds, N-B coordination bonds, and π-π stacking, along

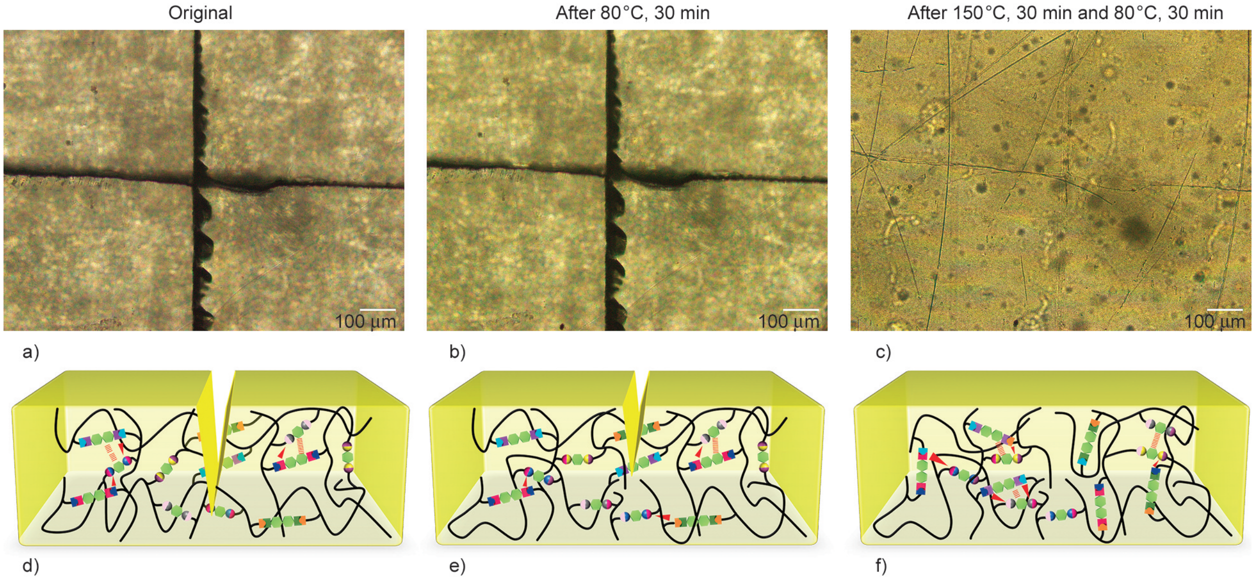

Figure 3. POM images of PB-8BO-8DA self-healing process, a) damaged, b) self-healed at 80 °C for 30 min, c) self-healed at 150 °C for 30 min followed by 120 min at 80 °C. Schemes of PB-8BO-8DA self-healing process: d) damaged, e) self-healed at 80 °C for 30 min, f) self-healed at 150 °C for 30 min followed by 120 min at 80 °C.

Table 2. Mechanical properties and self-healing ratio of the PB-BO-DA series materials.

Sample	Elongation at break [%]	Tensile strength [MPa]	Self-healing tensile strength [MPa]	Self-healing efficiency [%]
PB-8BO	61.4	1.24	1.23	99.5
PB-8BO-2DA	64.7	6.11	6.06	99.0
PB-8BO-4DA	57.9	8.11	8.64	100.0
PB-8BO-6DA	42.2	13.27	13.96	100.0
PB-8BO-8DA	29.0	16.46	16.55	100.0
PB-6BO-8DA	26.5	12.68	12.67	99.9
PB-4BO-8DA	36.8	5.88	6.54	100.0
PB-2BO-8DA	84.6	5.19	5.17	99.6
PB-8DA	141.6	2.32	2.39	100.0

with reversible Diels-Alder reactions within the dual-network structure.

The results of theoretical calculations involving the optimization of intermolecular interaction models and energy distribution calculations are shown in Figure 4d to provide a comprehensive understanding of the interactions between BDB and the Diels-Alder adduct [28–30]. In the Figure 4d, white, pink, gray, blue and red spheres represented H, B, C, N and O atoms, respectively. The green shadow represented π-π packing, while the blue shadow referred to the N-B coordination bond. The size and intensity of these shaded areas reflect the strength of these interactions. Based on the color distribution in Figure 4d, BDB and Diels-Alder adduct exhibited prominent N-B coordination bonds and extensive π-π stacking interactions, characterized by high-energy interactions. Specifically, the interaction energy between BDB and the Diels-Alder adduct was calculated to be 70.51 kJ/mol using the def2-TZVP basis set [30].

It is noteworthy that PB-8BO-8DA achieved very high tensile strength (16.46 MPa) and self-healing efficiency (99%), placing it among the top materials in the field of self-healing rubber [31–45]. This achievement is attributed to BO and DA double dynamic bond networks. PB cross-linked networks are all composed of dynamic covalent bonds. As a result, almost all dynamic bonds can realize dynamic reaction and generate new cross-linked networks after material damage. Thus, self-healing efficiency and tensile strength are enhanced simultaneously. Table 3 shows the results compared with other published studies.

3.4. Reprocessing properties

Recycling or reprocessing permanently cross-linked polymers is inherently difficult [46]. For verifying

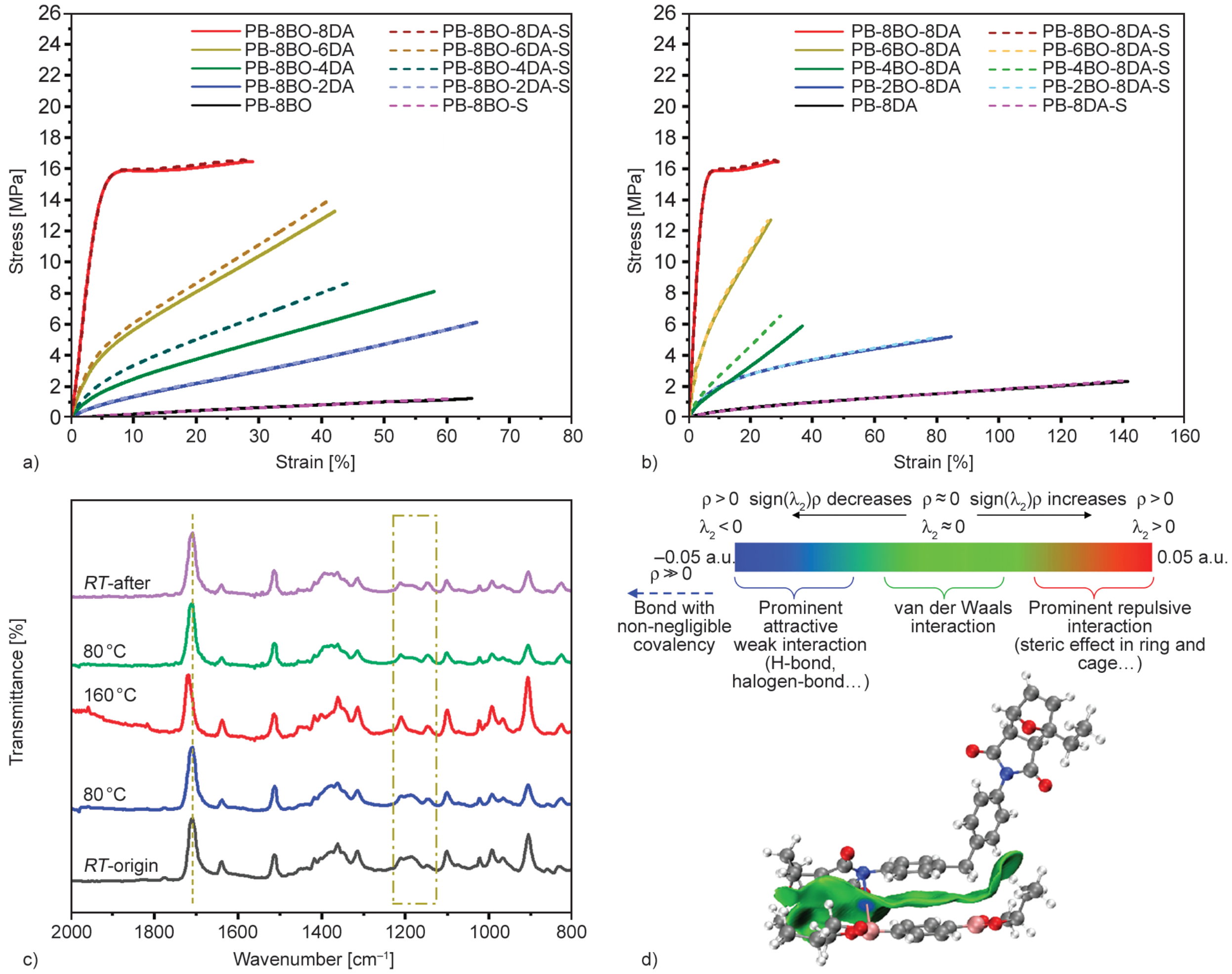

Figure 4. a) and b) The tensile curve and the corresponding self-healing curve of the dual-network elastomer with different B-O bond and DA bond content, c) FTIR spectra of PB-8BO-8DA samples at different temperatures, d) interactions for BDB and Diels Alder adduct.

Table 3. Comparison of some tensile strength data for dynamic bond elastomers with self-healing.

Elastic matrix	Dynamic bond	Tensile strength [MPa]	Self-healing ratio [%]	Reference
Polybutadiene	Hydrogen bond	1.02	98	[31]
Natural rubber	Hydrogen bond	6.50	80	[32]
Bromobutyl rubber	π-π packing	8.10	90	[33]
Epoxidized natural rubber	AP@Fe^{3+} interaction	2.23	87	[34]
Natural rubber	Zn^{2+} interaction	7.80	90	[35]
Polydimethylsiloxane	Imine	1.50	93	[36]
Polybutadiene	Imine + ionic hydrogen bonding	1.57	99	[37]
Styrene butadiene rubber	Boroxine	2.68	80	[38]
Epoxidized natural rubber	Disulfide	9.60	98	[39]
Natural rubber	Diels-Alder chemistry	1.47	85	[40]
Polybutadiene	Diels-Alder chemistry	5.59	90	[41]
Polydimethylsiloxane	Imine + boroxine	0.12	97.8	[42]
Epoxidized natural rubber	Disulfide + boroxine + imine	2.06	97	[43]
Epoxidized natural rubber	Boroxine + hydrogen bond	3.46	91.10	[44]
Epoxidized natural rubber	Disulfide + boroxine	6.30	82.87	[45]
Polybutadiene	Boroxine + Diels-Alder chemistry	16.46	99	This work

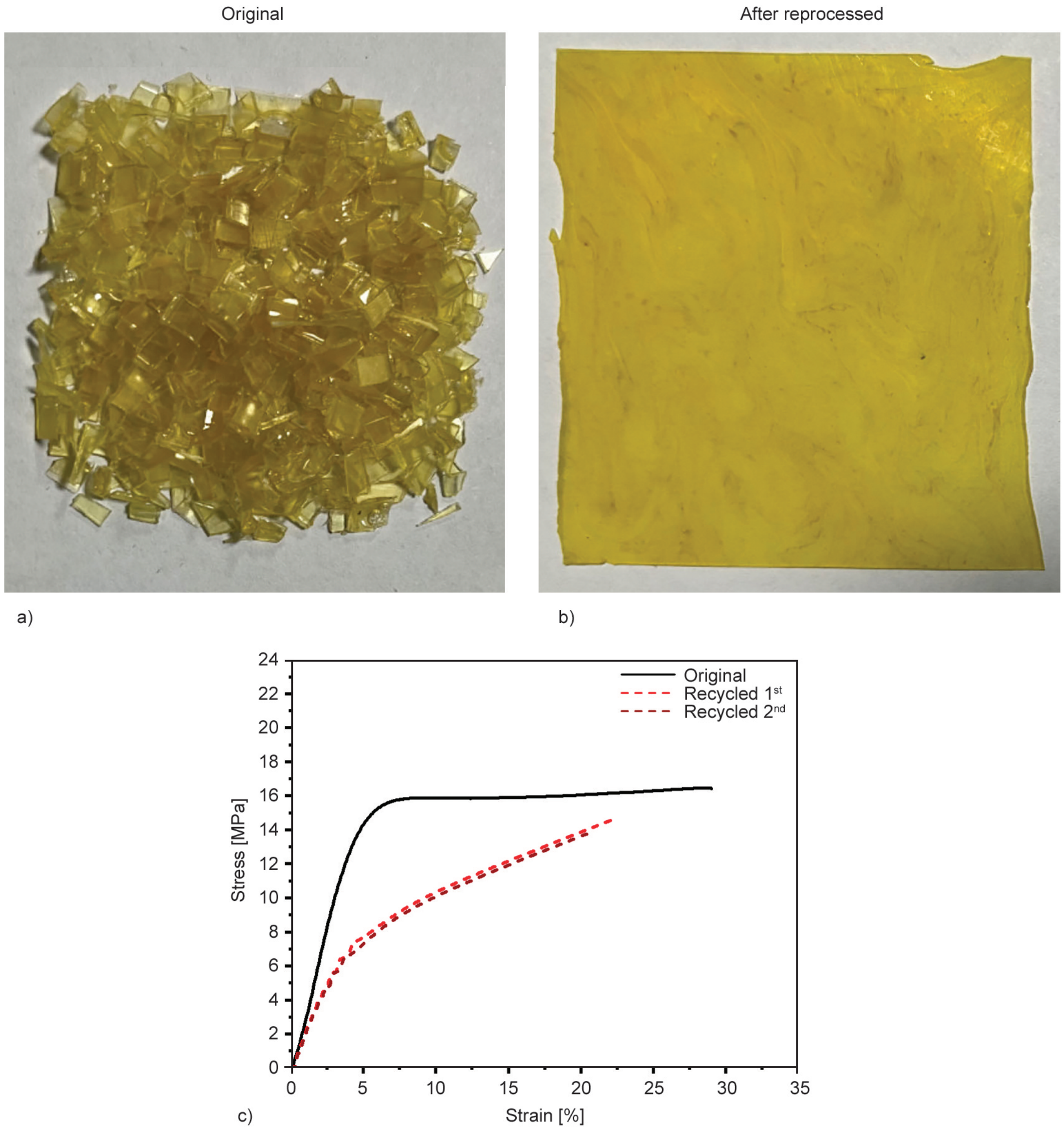

Figure 5. The original material (a) and the reprocessed sample (b). The stress-strain curves of the original, and the recycled materials (c).

the recyclability of the material, it was cut into pieces and gathered into a square mold, then hot pressed at 150 °C under 10 MPa for 30 min, followed by a 24 h hold at 80 °C to facilitate the reformation of dynamic bonds (Figures 5a and 5b). Tensile tests were carried out using dumbbell-shaped specimens to evaluate both mechanical and recyclable properties [15, 19, 35–38]. As shown in Figure 5c, the sample demonstrated repeated recoverability due to the exchange properties of the dynamic boronic ester bond and the dissociative reformation of the Diels-Alder bonds. After two cycles, the tensile curves of the sample almost overlapped, with the tensile strength reaching 13.81 MPa, achieving η_r = 84.3% recyclability.

3.5. Solid-state plasticity and dual shape memory property

Since the loss factor tanδ of PB-BO-DA appeared a distinct peak corresponding to the movement of the PB segment and partial dynamic bond reaction of PB-BO-DA. The dual thermal transition in PB-BO-DA rubber endowed it with high-temperature plasticity and shape memory capabilities [20, 32, 36]. To achieve shape change in PB-BO-DA, DA bonds with a higher thermal response temperature maintained the permanent shape, while T_g and B-O bonds exchange can be used to fix the temporary shape (Figure 6a). In order to investigate the shape memory property, the sample underwent step (1) to change to U temporary shape at 90 °C

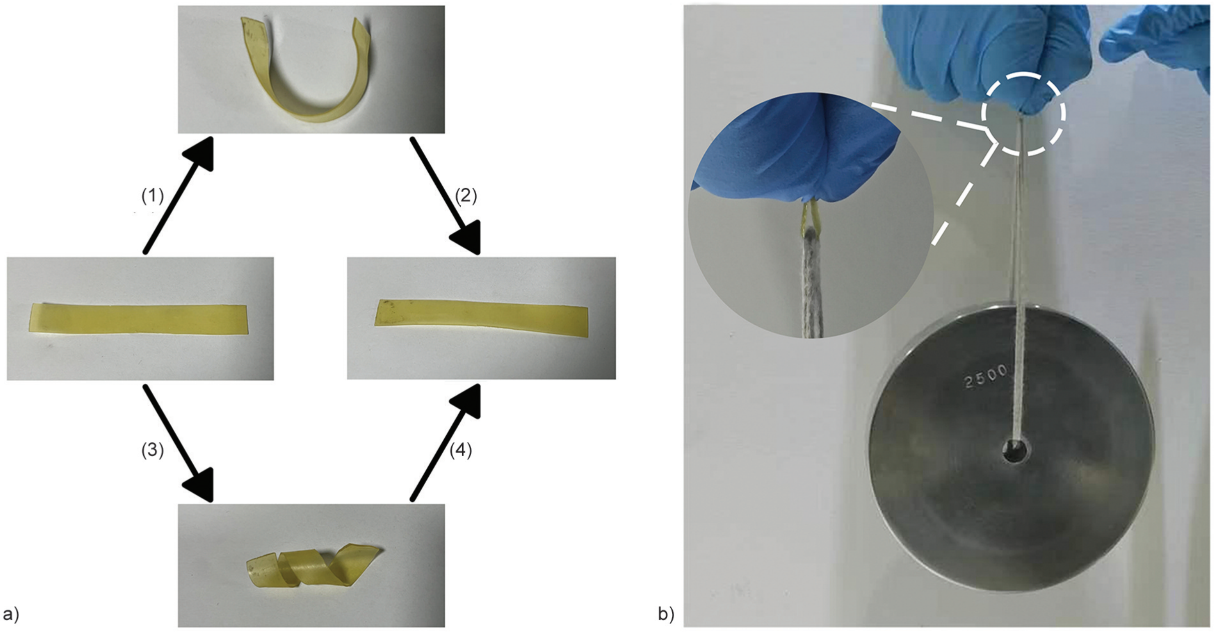

Figure 6. a) Photographs demonstrating the shape-memory behavior of the PB-8BO-8DA film. (1) heated to 90 °C while being deformed into a U shape and then cooled to –20 °C to fix the temporary shape, and (2) reheated to 90 °C to recover the permanent shape. (3) heated to 90 °C while being deformed into crimp shape and then cooled to –20 °C to fix the temporary shape, and (4) reheated to 90 °C to recover the permanent shape. b) 0.1 g of U temporary shape can lift 2500 g of weight.

(below the r-DA temperature, ensuring material solidity), then rapidly cooled to –20 °C (below T_g) to fix the shape, and then quickly restored the U temporary shape to original shape at 90 °C through step (2). Similarly, it can also be shaped into a crimped temporary shape and recovered to its original shape through steps (3) and (4). Finally, a sample weighing 0.1 g of PB-8BO-8DA in the U-shaped temporary form can lift a weight of 2500 g (Figure 6b).

4. Conclusions

In summary, polybutadiene dual dynamic network rubber was prepared by using dynamic boronic ester and Diels-Alder chemistry through a thiol-ene reaction. Based on the different content of double dynamic covalent bonds in the polybutadiene matrix, we have found that the Diels-Alder chemistry has less constraint on the rubber chain segment, and the dynamic borate ester bond significantly constrain the movement of the polybutadiene chain. Dual network polybutadiene rubber will not experience thermal weight loss within 200 °C. After treating the damaged double network rubber at different temperatures, we found that the borate ester bond underwent a dynamic exchange reaction at 90 °C, while the DA bond broke at 150 °C and reformed at 90 °C.

The dual network polybutadiene achieved a tensile strength of 16.46 MPa and a 99% self-healing efficiency attributed to the presence of numerous intermolecular interactions (π-π packing and N-B coordination bonds) through variable temperature FTIR and theoretical calculations. Moreover, the dual network polybutadiene recovered after hot pressing still has a tensile strength of 13.81 MPa. Ultimately, the dual network polybutadiene rubber also possesses thermoplastic properties and excellent shape memory capabilities, with its temporary shape capable of lifting weights up to 25 000 times its own weight. This work provides a simple strategy for the design and preparation of a large number of multifunctional polyolefin materials with high mechanical properties and high self-healing ability.

Acknowledgements

This work was supported by National Natural Science Foundation of China (U22A20144), Key Natural Science Foundation of Ningxia in China (2022AAC02017), and Key R&D projects of Ningxia in China(2019BFH02018).

References

[1] Xu J., Wang S., Wang G-J. N., Zhu C., Luo S., Jin L., Gu X., Chen S., Feig V. R., To J. W. F., Rondeau-Gagné S., Park J., Schroeder B. C., Lu C., Oh J. Y., Wang Y., Kim Y-H., Yan H., Sinclair R., Zhou D., Xue G., Murmann B., Linder C., Cai W., Tok J. B-H., Chung J. W., Bao Z.: Highly stretchable polymer semiconductor films through the nanoconfinement effect. Science, **355**, 59–64 (2017). https://doi.org/10.1126/science.aah4496

[2] Tadakaluru S., Thongsuwan W., Singjai P.: Stretchable and flexible high-strain sensors made using carbon nanotubes and graphite films on natural rubber. Sensors, **14**, 868–876 (2014). https://doi.org/10.3390/s140100868

[3] Tee B. C-K., Wang C., Allen R., Bao Z.: An electrically and mechanically self-healing composite with pressure- and flexion-sensitive properties for electronic skin application. Nature Nanotechnology, **7**, 825–832 (2012). https://doi.org/10.1038/nnano.2012.192

[4] Trovatti E., Lacerda T. M., Carvalho A. J. F., Gandini A.: Recycling tires? Reversible crosslinking of poly(butadiene). Advanced Materials, **27**, 2242–2245 (2015). https://doi.org/10.1002/adma.201405801

[5] Endo M., Noguchi T., Ito M., Takeuchi K., Hayashi T., Kim Y. A., Wanibuchi T., Jinnai H., Terrones M., Dresselhaus M. S.: Extreme-performance rubber nanocomposites for probing and excavating deep oil resources using multi-walled carbon nanotubes. Advanced Functional Materials, **18**, 3403 (2008). https://doi.org/10.1002/adfm.200801136

[6] Jiang K., Shi J., Ge Y., Zou R., Yao P., Li X., Zhang L.: Complete devulcanization of sulfur-cured butyl rubber by using supercritical carbon dioxide. Journal of Applied Polymer Science, **127**, 2397–2406 (2012). https://doi.org/10.1002/app.37542

[7] Chen Y., Kushner A. M., Williams G. A., Guan Z.: Multiphase design of autonomic self-healing thermoplastic elastomers. Nature Chemistry, **4**, 467–472 (2012). https://doi.org/10.1038/nchem.1314

[8] Cordier P., Tournilhac F., Soulié-Ziakovic C., Leibler L.: Self-healing and thermoreversible rubber from supramolecular assembly. Nature, **451**, 977–980 (2008). https://doi.org/10.1038/nature06669

[9] Das A., Sallat A., Böhme F., Suckow M., Basu D., Wießner S., Stöckelhuber K. W., Voit B., Heinrich G.: Ionic modification turns commercial rubber into a self-healing material. ACS Applied Materials and Interfaces, **7**, 20623–20630 (2015). https://doi.org/10.1021/acsami.5b05041

[10] Li C-H., Wang C., Keplinger C., Zuo J-L., Jin L., Sun Y., Zheng P., Cao Y., Lissel F., Linder C., You X-Z., Bao Z.: A highly stretchable autonomous self-healing elastomer. Nature Chemistry, **8**, 618–624 (2016). https://doi.org/10.1038/nchem.2492

[11] Bode S., Zedler L., Schacher F. H., Dietzek B., Schmitt M., Popp J., Hager M. D., Schubert U. S.: Self-healing polymer coatings based on crosslinked metallosupramolecular copolymers. Advanced Materials, **25**, 1634–1638 (2013). https://doi.org/10.1002/adma.201203865

[12] Burattini S., Greenland B. W., Merino D. H., Weng W., Seppala J., Colquhoun H. M., Hayes W., Mackay M. E., Hamley I. W., Rowan S. J.: A healable supramolecular polymer blend based on aromatic π-π stacking and hydrogen-bonding interactions. Journal of the American Chemical Society, **132**, 12051–12058 (2010). https://doi.org/10.1021/ja104446r

[13] Burattini S., Colquhoun H. M., Fox J. D., Friedmann D., Greenland B. W., Harris P. J. F., Hayes W., Mackay M. E., Rowan S. J.: A self-repairing, supramolecular polymer system: Healability as a consequence of donor-acceptor π-π stacking interactions. Chemical Communications, **2009**, 6717–6719 (2009). https://doi.org/10.1039/b910648k

[14] Lai Y., Kuang X., Zhu P., Huang M., Dong X., Wang D.: Colorless, transparent, robust, and fast scratch-self-healing elastomers *via* a phase-locked dynamic bonds design. Advanced Materials, **30**, 1802556 (2018). https://doi.org/10.1002/adma.201802556

[15] Xiang H. P., Qian H. J., Lu Z. Y., Rong M. Z., Zhang M. Q.: Crack healing and reclaiming of vulcanized rubber by triggering the rearrangement of inherent sulfur crosslinked networks. Green Chemistry, **17**, 4315–4325 (2015). https://doi.org/10.1039/c5gc00754b

[16] Lai J-C., Mei J-F., Jia X-Y., Li C-H., You X-Z., Bao Z.: A stiff and healable polymer based on dynamic-covalent boroxine bonds. Advanced Materials, **28**, 8277–8282 (2016). https://doi.org/10.1002/adma.201602332

[17] Lei X., Huang Y., Liang S., Zhao X., Liu L.: Preparation of highly transparent, room-temperature self-healing and recyclable silicon elastomers based on dynamic imine bond and their ion responsive properties. Materials Letters, **268**, 127598 (2020). https://doi.org/10.1016/j.matlet.2020.127598

[18] Bao C., Jiang Y-J., Zhang H., Lu X., Sun J.: Room-temperature self-healing and recyclable tough polymer composites using nitrogen-coordinated boroxines. Advanced Functional Materials, **28**, 1800560 (2018). https://doi.org/10.1002/adfm.201800560

[19] Chen X., Dam M. A., Ono K., Mal A., Shen H., Nutt S. R., Sheran K., Wudl F.: A thermally re-mendable cross-linked polymeric material. Science, **295**, 1698–1702 (2002). https://doi.org/10.1126/science.1065879

[20] Deng M., Guo F., Liao D., Hou Z., Li Y.: Aluminium-catalyzed terpolymerization of furfuryl glycidyl ether with epichlorohydrin and ethylene oxide: Synthesis of thermoreversible polyepichlorohydrin elastomers with furan/maleimide covalent crosslinks. Polymer Chemistry, **9**, 98–107 (2018). https://doi.org/10.1039/c7py01516j

[21] Montarnal D., Tournilhac F., Hidalgo M., Couturier J-L., Leibler L.: Versatile one-pot synthesis of supramolecular plastics and self-healing rubbers. Journal of the American Chemical Society, **131**, 7966–7967 (2009). https://doi.org/10.1021/ja903080c

[22] Wu J., Cai L-H., Weitz D. A.: Tough self-healing elastomers by molecular enforced integration of covalent and reversible networks. Advanced Materials, **29**, 1702616 (2017). https://doi.org/10.1002/adma.201702616

[23] Yang Y., Huang L., Wu R., Fan W., Dai Q., He J., Bai C.: Assembling of reprocessable polybutadiene-based vitrimers with high strength and shape memory *via* catalyst-free imine-coordinated boroxine. ACS Applied Materials and Interfaces, **12**, 33305–33314 (2020). https://doi.org/10.1021/acsami.0c09712

[24] Zhao J., Xu R., Luo G., Wu J., Xia H.: Self-healing poly(siloxane-urethane) elastomers with remoldability, shape memory and biocompatibility. Polymer Chemistry, **7**, 7278–7286 (2016). https://doi.org/10.1039/c6py01499b

[25] Bai J., He Q., Shi Z., Tian M., Xu H., Ma X., Yin J.: Self-assembled elastomer nanocomposites utilizing C60 and poly(styrene-b-butadiene-*b*-styrene) *via* thermally reversible Diels-Alder reaction with self-healing and remolding abilities. Polymer, **116**, 268–277 (2017). https://doi.org/10.1016/j.polymer.2017.03.080

[26] Bekas D. G., Tsirka K., Baltzis D., Paipetis A. S.: Self-healing materials: A review of advances in materials, evaluation, characterization and monitoring techniques. Composites Part B: Engineering, **87**, 92–119 (2016). https://doi.org/10.1016/j.compositesb.2015.09.057

[27] Araya-Hermosilla R., Broekhuis A. A., Picchioni F.: Reversible polymer networks containing covalent and hydrogen bonding interactions. European Polymer Journal, **50**, 127–134 (2014). https://doi.org/10.1016/j.eurpolymj.2013.10.014

[28] Crisenza G. E. M., Mazzarella D., Melchiorre P.: Synthetic methods driven by the photoactivity of electron donor-acceptor complexes. Journal of the American Chemical Society, **142**, 5461–5476 (2020). https://doi.org/10.1021/jacs.0c01416

[29] Brals J., McGuire T. M., Watson A. J. B.: A chemoselective polarity-mismatched photocatalytic C(sp^3)-C(sp^2) cross-coupling enabled by synergistic boron activation. Angewandte Chemie International Edition, **62**, e202310462 (2023). https://doi.org/10.1002/anie.202310462

[30] Wang J., He T., Li P., Meng L., Ding Y., Tian H., Bai H., Lou X., Zhang H.: An *in situ* thermal cross-linking binder for silicon-based lithium ion battery. Journal of Colloid and Interface Science, **649**, 795–803 (2023). https://doi.org/10.1016/j.jcis.2023.06.158

[31] Wang D., Guo J., Zhang H., Cheng B., Shen H., Zhao N., Xu J.: Intelligent rubber with tailored properties for self-healing and shape memory. Journal of Materials Chemistry A, **3**, 12864–12872 (2015). https://doi.org/10.1039/c5ta01915j

[32] Shen Q., Wu M., Xu C., Wang Y., Wang Q., Liu W.: Sodium alginate crosslinked oxidized natural rubber supramolecular network with rapid self-healing at room temperature and improved mechanical properties. Composites Part A: Applied Science and Manufacturing, **150**, 106601 (2021). https://doi.org/10.1016/j.compositesa.2021.106601

[33] Zhang L., Wang H., Zhu Y., Xiong H., Wu Q., Gu S., Liu X., Huang G., Wu J.: Electron-donating effect enabled simultaneous improvement on the mechanical and self-healing properties of bromobutyl rubber ionomers. ACS Applied Materials and Interfaces, **12**, 53239–53246 (2020). https://doi.org/10.1021/acsami.0c14901

[34] Cao L., Gong Z., Liu C., Fan J., Chen Y.: Design and fabrication of mechanically strong and self-healing rubbers *via* metal-ligand coordination bonds as dynamic crosslinks. Composites Science and Technology, **207**, 108750 (2021). https://doi.org/10.1016/j.compscitech.2021.108750

[35] Wu M., Luo T., Lu J., Wang Y., Lin B., Xu C.: Fabricating robust natural rubber composites with photothermal conversion and near-infrared light-actuated remote-controlled accurate self-healing. Composites Science and Technology, **235**, 109966 (2023). https://doi.org/10.1016/j.compscitech.2023.109966

[36] Feng Z., Yu B., Hu J., Zuo H., Li J., Sun H., Ning N., Tian M., Zhang L.: Multifunctional vitrimer-like polydimethylsiloxane (PDMS): Recyclable, self-healable, and water-driven malleable covalent networks based on dynamic imine bond. Industrial and Engineering Chemistry Research, **58**, 1212–1221 (2019). https://doi.org/10.1021/acs.iecr.8b05309

[37] Zhang H., Wang D., Wu N., Li C., Zhu C., Zhao N., Xu J.: Recyclable, self-healing, thermadapt triple-shape memory polymers based on dual dynamic bonds. ACS Applied Materials and Interfaces, **12**, 9833–9841 (2020). https://doi.org/10.1021/acsami.9b22613

[38] Chen Y., Tang Z., Zhang X., Liu Y., Wu S., Guo B.: Covalently cross-linked elastomers with self-healing and malleable abilities enabled by boronic ester bonds. ACS Applied Materials and Interfaces, **10**, 24224–24231 (2018). https://doi.org/10.1021/acsami.8b09863

[39] Cheng B., Lu X., Zhou J., Qin R., Yang Y.: Dual cross-linked self-healing and recyclable epoxidized natural rubber based on multiple reversible effects. ACS Sustainable Chemistry and Engineering, **7**, 4443–4455 (2019).
https://doi.org/10.1021/acssuschemeng.8b06437

[40] Tanasi P., Santana M. H., Carretero-González J., Verdejo R., López-Manchado M. A.: Thermo-reversible cross-linked natural rubber: A Diels-Alder route for reuse and self-healing properties in elastomers. Polymer, **175**, 15–24 (2019).
https://doi.org/10.1016/j.polymer.2019.04.059

[41] Bai J., Li H., Shi Z., Yin J.: An eco-friendly scheme for the cross-linked polybutadiene elastomer *via* Thiol-Ene and Diels-Alder click chemistry. Macromolecules, **48**, 3539–3546 (2015).
https://doi.org/10.1021/acs.macromol.5b00389

[42] Wang P., Wang Z., Liu L., Ying G., Cao W., Zhu J.: Self-healable and reprocessable silicon elastomers based on imine-boroxine bonds for flexible strain sensor. Molecules, **28**, 6049 (2023).
https://doi.org/10.3390/molecules28166049

[43] Liu W., Huang J., Gong Z., Fan J., Chen Y.: Healable, recyclable and mechanically robust elastomers with multiple dynamic cross-linking bonds. Polymer, **252**, 124900 (2022).
https://doi.org/10.1016/j.polymer.2022.124900

[44] Ye T., Kuang D., Han W., Yin Y., Wang C.: Room-temperature self-healing graphene/rubber-based supramolecular elastomers utilized by dynamic boroxines and hydrogen bonds for human motion detection. Colloids and Surfaces A: Physicochemical and Engineering Aspects, **657**, 130411 (2023).
https://doi.org/10.1016/j.colsurfa.2022.130411

[45] Jiang Q., Gao Y., Liao L., Yu R., Liao J.: Biodegradable natural rubber based on novel double dynamic covalent cross-linking. Polymers, **14**, 1380 (2022).
https://doi.org/10.3390/polym14071380

[46] Yang Y., Huang L., Wu R., Niu Z., Fan W., Dai Q., Cui L., He J., Bai C.: Self-strengthening, self-welding, shape memory, and recyclable polybutadiene-based material driven by dual-dynamic units. ACS Applied Materials and Interfaces, **14**, 3344–3355 (2022).
https://doi.org/10.1021/acsami.1c23007